Essential role of residual stress in fiber optic extrinsic Fabry-Perot sensors for detecting the acoustic signals of partial discharges

WENRONG SI[a,#], HAOYONG LI[b,c,#], CHENZHAO FU[a], PENG YUAN[d], YITING YU[b,c,*]
[a]*State Grid Shanghai Electric Power Research Institute, Shanghai 200437, P. R. China*
[b]*Key Laboratory of Micro/Nano Systems for Aerospace (Ministry of Education), Northwestern Polytechnical University, Xi'an 710072, P. R. China*
[c]*Key Laboratory of Micro- and Nano-Electro-Mechanical Systems of Shaanxi Province, Northwestern Polytechnical University, Xi'an 710072, P. R. China*
[d]*Xi'an Maorong Power Equipment Co., Ltd., Xi'an 710048, P. R. China*
#: These authors contribute equally to this research

The effects of residual stress on fiber optic extrinsic Fabry-Perot interferometric (EFPI) sensors for detecting the acoustic signals of partial discharges (PDs) were investigated using the finite element method (FEM). Results indicate that the residual stress in the vibrational membrane may change the natural frequency of the membrane, which would subsequently cause the deviation in the designed performance of the EFPI sensor, including the responsive displacement of the membrane, as well as the sensitivity and resolution of the sensor. According to the design, when the residual stress in the membrane exists, the residual tensile stress makes the responsive sensitivity of the membrane for the EFPI sensor to be increased by 0.017 nm/kPa/MPa (on average) and resolution to be decreased by 0.07 Pa/MPa, while the residual compressive stress takes effect oppositely, as -0.008 nm/kPa/MPa and +0.085 Pa/MPa, respectively.

(Received February 7, 2017; accepted November 28, 2017)

Keywords: Fabry-Perot sensors, Residual stress, Vibrational membrane, Partial discharges

1. Introduction

Partial discharge (PD) detection in the power transformers is a crucial part for the power industry. The occurrence of PDs within transformers implies an insulation breakdown, which may lead to the large personnel injury and property damage. For example, a single transformer failure caused by PDs will result in at least $10 million economic loss [1].

The use of electrical, chemical, and acoustic measurements to detect PDs inside power transformers has been extensively studied. However, the electrical method is not suitable to be applied in the field for in-service transformers due to the high level of electromagnetic interference (EMI), and the chemical method exists a long delay between the initiation of a PD source and the appearance of the PD signal to be detectable. Furthermore, in order to determine the exact location of a detected PD source, which is also quite important for the practical application in the PD study [2], both the electrical and chemical methods seem impossible. In general, a PD leads to a localized, nearly instantaneous release of energy, and the ultrasonic waves are then produced and propagate in the power transforms. Thus, an acoustic sensor can be used to detect PDs and provides a better noise immunity for the on-line PD detection [3, 4]. Furthermore, the acoustic method can be effectively utilized to locate the position of a PD source, as the phase delay or the amplitude attenuation is caused during the propagating procedure of the acoustic waves.

In general, one can use the piezoelectric acoustic sensors to detect the PDs by fixing them externally on the walls of a power transformer. However, two possible disadvantages associated with an externally mounted piezoelectric sensor should be considered. One is the degeneration of the signal-to-noise ratio caused by the environmental noises, e.g. EMI and corona effects. The other is the difficulty in accurately positioning PDs because of the multiple paths of acoustic wave transmission [5]. Therefore, the sensors that can be put inside a transformer and even deep within the transformer, are urgently needed to pick up the clean PD-induced acoustic signals. In the meanwhile, taking regard to the safety and easy installation, these sensors have to be chemically inert, electrically insulating, passive, and small in size. For this purpose, optical fiber-based sensors become ideal candidates for measuring a wide range of chemical and physical parameters. They reveal a number

of inherent advantages, e.g. high frequency response, high sensitivity, light weight, small size, electrical insulation, and immunity to EMI noise, all making the optical fiber sensors an excellent choice for the PD detection. In recent years, fiber optic extrinsic Fabry-Perot interferometric (EFPI) sensors are widely employed for the acoustic signal detection [6-9].

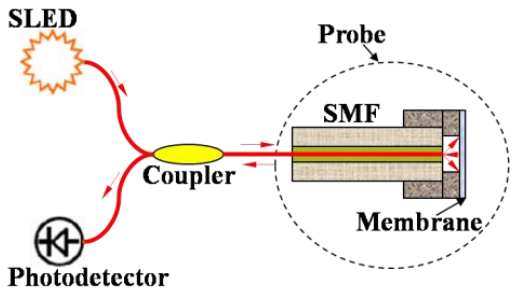

Fig. 1. Schematic of a fiber optic EFPI sensor system

Fig. 1 shows the schematic of the whole fiber optic EFPI sensor system. The system is composed of a single-mode fiber (SMF), a superluminescent light emitting diode (SLED) or LED, a fiber optic coupler, a low-noise optical receiver (photodetector), and most importantly, a sensor probe. In the system, a laser source (wavelength of 1310 nm) is used as the light source, and an optical signal is converted to an electrical signal by the photodetector. The light is launched into the sensor through the coupler, and the SMF is used to link the sensor and the optical receiver, and the reflected light from the sensor is transmitted back through the coupler to the photodetector. The probe of PD sensors is based on the Fabry–Perot interferometer that consists of a reflective membrane and the end face of the SMF. The applied pressure generated by the PDs causes a structural deflection of the membrane, and thus the cavity length, which can be detected by an appropriate optical interrogation technique [10, 11].

As an important sensing element, the membrane plays a key role in the performance of the fiber optic EFPI sensors [12, 13]. However, the residual stress in the membrane can be caused not only by the mismatch in the coefficient of thermal expansion because the fabrication of current fiber optic EFPI sensors usually involves several materials, but also by the temperature-related fabrication processes of the membrane, which is difficult to be totally eliminated [14, 15]. In recent years, we have carried out a large number of experimental tests on the residual stress in the micromechanical thin films, resulting in the discovery that both the residual tensile and compressive stresses in the high-quality membranes should not be more than 400MPa for most cases [16].

In this paper, the effects of residual stress on the fiber optic EFPI sensor, including the natural frequency and responsive displacement of the membrane, and the resolution and sensitivity of the final sensor, were investigated using the finite element method (FEM) [17]. The results are useful for the design of a sensor system capable of successfully monitoring the PD activities in power transformers as well as other acoustic events.

2. Results and discussions

Residual stress in the membrane can change the stiffness of the membrane structure, which would subsequently cause the deviation of its natural frequency. In the meantime, the desired natural frequency of the membrane, as a key performance parameter for the EFPI sensor, depends on the frequency spectrum of the ultrasonic wave generated by the PDs, and the change of it may result in the variation of the responsive displacement of the vibrational membrane, as well as the sensitivity and resolution of the ultimately achieved EFPI sensor.

2.1. Natural frequency of the membrane

The determination of natural frequency of the membrane depends on the frequency spectrum of the ultrasonic wave generated by the PDs. Experimental and theoretical analysis show that the ultrasonic frequency spectrum energy of PDs is normally concentrated in the range of 20-300 kHz. However, the noise frequency distribution of the usual transformers is less than 65 kHz and the absorption coefficient of the medium to the ultrasonic wave is quadratically proportional to the frequency, that is, the higher the frequency, the greater the absorption coefficient, and thus the more powerful attenuation of the ultrasonic wave in the procedure of transmission. Therefore, the natural frequency of the membrane is generally selected in the range of 70-180 kHz. Normally, the membrane material is silicon or fused-silica [18]. Silicon as a membrane material has a number of advantages, including the relatively mature micromachining technology, high fabrication accuracy, easy to produce the insulating film, and with an abundant natural resource. These advantages make silicon an excellent candidate for the fiber optic EFPI sensor. In this work, silicon membrane with the thickness of 100 μm and the diameter of 3 mm is adopted. FEM simulation with the ANSYS software (ver. 14.5) shows that the natural frequency of the membrane is around 169 kHz. For silicon, the Young's modulus is 163 GPa at 25°C, Poisson's ratio is 0.22, coefficient of thermal expansion is 2.6×10^{-6} /℃ and density is 2330 kg/m^3.

The experimental results show that the mechanical and thermal effects are the important factors to cause the residual stress [19]. Because of the fabrication processing, the residual stress is inevitably existing, yet still difficult to be accurately determined both in theory and experimental measurement. At present, there are two main methods to load the residual stress in the membrane by the FEM in ANSYS: the direct command method and the equivalent

thermal stress method. However, the direct command method requires a clear understanding of the existence of residual stress, otherwise the model will deviate from the actual situation greatly. The equivalent thermal stress method is relatively simple and effective, which can be expressed by

$$\sigma_t = \frac{E}{1-\mu^2} \bullet \alpha \bullet \Delta T \quad (1)$$

where σ_t is the equivalent thermal stress, E, μ and α is the elastic modulus, Poisson's ratio, and coefficient of thermal expansion of the membrane material, respectively, and ΔT denotes the temperature change. Therefore, the thermal stress can be effectively loaded with an easy way in the simulation by introducing a temperature difference to behave as the effective residual stress, ancd then, its effect on the mechanical properties of the membranes can be investigated. The same method was successfully employed in our previous research [16], which will be also adopted for designing the fiber optic EFPI sensor. In this paper, the whole analysis procedure using ANSYS (Ver. 14.5) mainly includes the simulation of steady-state thermal, static structural, modal and harmonic response, and there is only one initial boundary condition used for all these analyses, which means that the circumferential side of membrane is fixed. The specific procedure is as follows:

First, the membrane was modeled in the three-dimensional Cartesian coordinate system, and the meshed elements of the membrane were generated by the automatic method under the mechanical physics preference, and the element quality and the element number are 0.9 and 3612, respectively. Then, the heat flux perpendicular to the membrane surface was applied to generate the desired thermal stress by accurately setting the overall temperature change. Finally, the membrane went through the pre-stressed modal analysis to calculate the natural frequency. For example, when the heat flux and ΔT were set to 100 W/m^2 and 100 °C, respectively, the equivalent thermal stress and natural frequency was 190 MPa and 177 kHz, respectively, and the distribution of the principal stress victor is shown in Fig. 2. According to our previous research experience, both the residual tensile and compressive stresses in the membranes with controlled micromachining processes are mostly less than 400MPa [16]. As a result, in this paper, the residual tensile stress and compressive stress within this range were discussed. Consequently, in the simulation, the heat flux was still set to 100 W/m^2, and the range of temperature change was applied from -260 °C to 275 °C. The final results, as shown in Fig. 3, reveal that the natural frequency is linearly increased by about 0.044 kHz/MPa as the residual tensile stress increasing and is linearly decreased by about 0.039 kHz/MPa with the increase of the residual compressive stress.

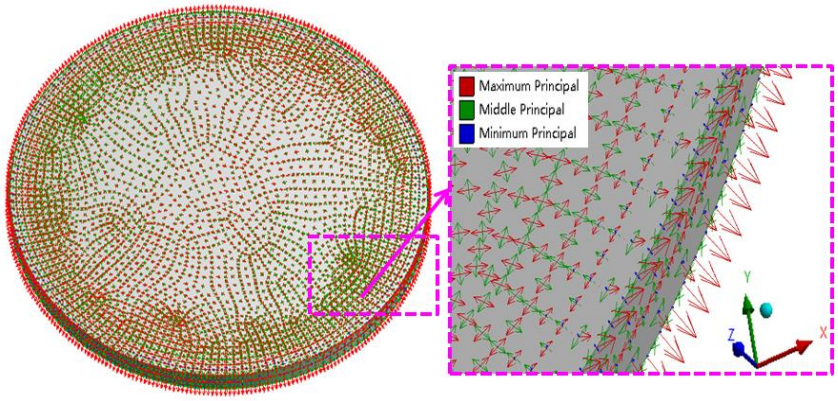

Fig. 2. The distribution of the principal stress victor with ΔT=100 °C. The inset gives an enlarged view

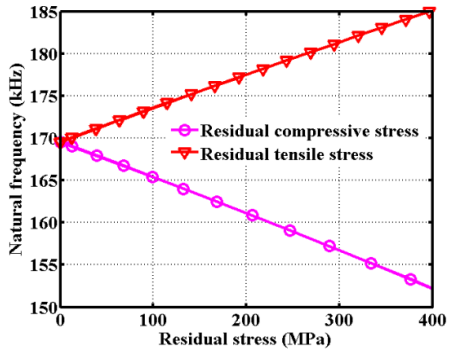

Fig. 3. The effects of residual stress on the natural frequency of the membrane

2.2. Central deflection of the membrane

As we know, the deviation of natural frequency under a certain residual stress will directly influence the central deflection of the membrane. Though ultrasonic signals generated by the PDs are mainly random and the spectrum is difficult to predict, the frequency range of the ultrasonic signal spectrum stays within the relatively assured range and the main change lies in the peak frequency. Normally, ultrasonic waves loaded on the membrane have the form of intermittent vibration. In general, the larger the discharge and the closer the distance to the PD source are, the greater the sound pressure will be. However, at a meter's distance away, the root-mean-square sound

pressure from a 10^{-12} C discharge is only 0.02 Pa due to the serious attenuation of ultrasonic wave in the power transformers [13, 20]. Nevertheless, the EFPI senor is prone to suffer from a few kPa, even dozens of kPa sound pressure, considering its operation in the transformer and also the possible location very close to the PD source as the arrangement of a large number of EFPI sensors is feasible due to their small volume and low cost [19-20]. Therefore, in order to analyze the effects of residual stress on the central deflection of the membrane, harmonic analysis was performed for the frequency ranging from 120 to 210 kHz, which is mostly interested for the PD detection, under a sinusoidal acoustic wave of p=9 kPa, 10 kPa, and 11 kPa, respectively [13]. The vibrating acoustic waves were applied onto the surface of the membrane.

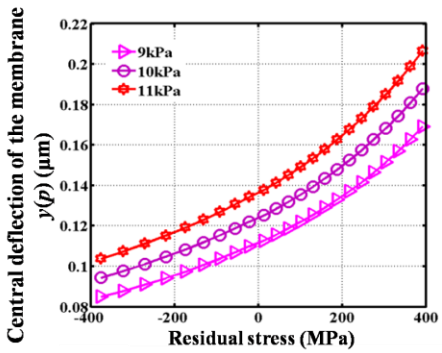

Fig. 4. The central deflection of the membrane under a sinusoidal acoustic wave of p=9 kPa, 10 kPa, and 11 kPa, respectively. The residual tensile stress is positive, and the residual compressive stress is negative

The results, as shown in Fig. 4, present that the central deflection of the membrane $y(p)$ is decreased by about 0.08 nm/MPa with the increasing of the residual compressive stress and is increased by about 0.16 nm/MPa as the residual tensile stress increasing. The central deflection of the membrane is linearly increased with respect to the applied pressure, especially when the deflection is less than 25% of the membrane thickness according to our simulation results. In such situations, the residual stress does not affect the intrinsic relationship between the central deflection of the membrane and the applied pressure p.

2.3. Resolution and sensitivity of the EFPI sensor

When the EFPI sensor works, according to the principle of the Fabry–Perot interferometer, the received light intensity Ir can be expressed by

$$I_r = I_0 \frac{R_1 + R_2 - 2\sqrt{R_1 R_2}\cos(\varphi)}{1 + R_2 R_1 - 2\sqrt{R_2 R_1}\cos(\varphi)} \tag{2}$$

where I_0 is the power of laser source, and φ is the round trip phase shift of the light inside the air cavity, which can be further described by

$$\varphi = \frac{4\pi nL}{\lambda} \tag{3}$$

where λ is the wavelength of light source, n is the refractive index of air (n=1), and L is the length of the air cavity.

As a result, we can plot the detected light intensity versus the cavity length L, as shown in Fig. 6, where R_1=0.04 is the reflectivity of the SMF's end face, R_2=0.9 is the reflectivity of the inner surface of the membrane, and λ=1310 nm, and the initial intensity of the laser source I_0 is assumed to 1.

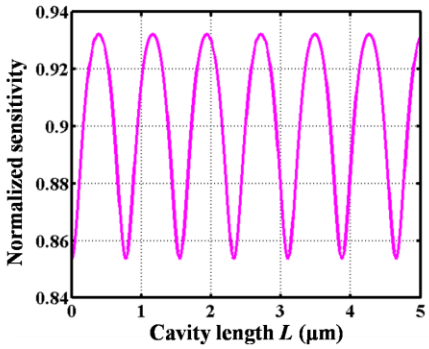

Fig. 5. The relationship between the normalized intensity and cavity length

From the Fig. 5, the detected light intensity varies periodically corresponds to the change of cavity length in the period of $\lambda/2$. It is due to the constructive and destructive interference of the multiple reflected lights inside the fiber. In general, the length between two adjacent intensity peaks or the valleys of the interference fringe is selected as the initial Fabry–Perot cavity length, and the region between the adjacent peak and valley is treated as the operating region which is $\lambda/4$ in length. In this approximately linear region, the output signal $V(p)$ of the sensor is proportional to the ultrasonic pressure p, expressed by

$$V(p) = S_T \bullet p \tag{4}$$

where S_T is the total sensitivity of the sensor, given by

$$S_T = S_\infty S_d = \alpha \bullet G \bullet R \bullet S_0 \bullet S_d \tag{5}$$

where α is the coupling coefficient of the light path (from the light source to the sensor and from the sensor to the receiver), G is for the optical fiber receiver, R is the responsive sensitivity for the photodetector, S_0 is the fringe sensitivity given by the slope in the linear region, and S_d is the responsive sensitivity of the membrane, expressed by

$$S_d = \frac{y(p)}{p} \tag{6}$$

According to Eqs. (4) and (5), the deviation of the membrane deflection caused by the residual stress will ultimately result in the shift of the membrane's responsive sensitivity S_d, and as a result, the sensor's total sensitivity S_T. However, the absolute deflection of the membrane depends on the level of discharges and the distance of the EFPI sensor to the source.

Fig. 6 shows the relationship of the responsive sensitivity S_d of the membrane versus residual stress, as well as the slope of it. The responsive sensitivity of the membrane is increased a bit more obviously (0.017 nm/kPa/MPa on average) as the residual tensile stress increasing, and is decreased slowly (0.008 nm/kPa/MPa on average) as the residual compressive stress increasing.

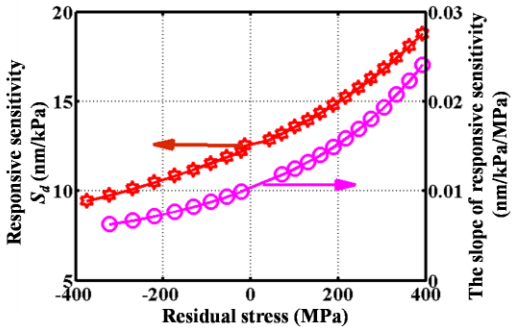

Fig. 6. The effect of residual stress on the responsive sensitivity S_d of the membrane

Therefore, the total sensitivity S_T of the sensor can be changed by

$$S_T = \alpha \bullet G \bullet R \bullet S_0 \bullet (S_d \pm \Delta S) = k(S_d \pm \Delta S) \tag{7}$$

where ΔS is the change of the membrane's responsive sensitivity caused by the residual stress, and k is the product of the responsive sensitivity of the other sensor elements in the whole system.

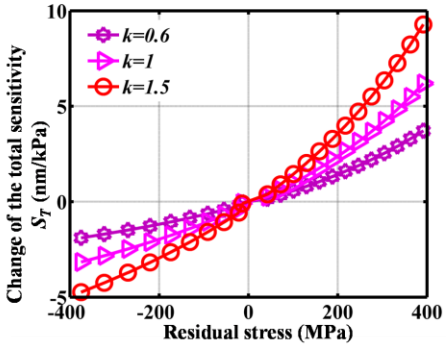

Fig. 7. The change of the sensor's sensitivity versus residual stress for different values of k

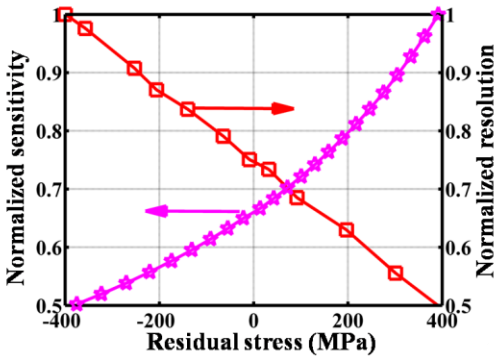

Fig. 8. The membrane's normalized sensitivity and resolution versus residual stress

In a word, residual stress in the membrane can cause the deviation of the total sensitivity of the sensor. The variation depends on the property of the residual stress and the product of the other responsive sensitivity k, and the greater the k, the greater the change of the total sensitivity of the sensor, as shown in Fig. 7. However, the rate of change versus residual stress is constant, as shown in Fig. 9.

The resolution of the membrane is a primary factor in determining the sensor's resolution, which is defined by the smallest displacement of the membrane that makes the sensor give an obvious output, and the resolution of the same membrane for the EFPI sensors with different accessories may be different. Therefore, Fig. 8 only gives the normalized membrane's resolution versus residual stress. In general, selecting the appropriate components for the sensor system, the ultrasonic signals can be measured, as long as the responsive displacement of the membrane is greater than 1 nm, and the results show that the membrane's resolution is decreased by about 0.07 Pa/MPa with the increase of the residual tensile stress and is increased by about 0.085 Pa/MPa as the residual compressive stress increasing.

3. Conclusions

The effects of residual stress in the membrane of the fiber optic EFPI sensor for detecting the acoustic signals of PDs are investigated using the finite element simulation. The results show that the natural frequency of the membrane is decreased linearly with the increase of the residual compressive stress and is increased linearly as the residual tensile stress increasing, resulting in the deviation of the responsive displacement of the membrane, and finally, the resolution and sensitivity of the sensor. The excessive residual stress in the membrane will lead to serious deviation of the designed parameters of the fiber optic EFPI sensor. As a result, the residual stress of the membrane is proposed to be under well control in order to achieve the desired device performance before the

assembly of the sensor. The results are useful for the design of the sensor system that is capable of successfully monitoring the PD activities in power transformers as well as the other acoustic events.

Acknowledgement

We acknowledge the financial sponsorship from the State Grid Shanghai Municipal Electric Power Company and the 111 Project (Grant No. B13044) for this research.

References

[1] B. Yu, D. W. Kim, J. Deng, H. Xiao, A. B. Wang, Appl. Opt. **42**(16), 3241 (2003).
[2] Y. Inoue, K. Suganuma, M. Kamba, M. Kikkawa, IEEE T. Power Deliver **5**(1), 226 (1990).
[3] L. E Lundgaard, IEEE Electr. Insul. Mag. **8**(4), 25 (1992).
[4] L. E. Lundgaard, IEEE Electr. Insul. Mag. **8**(5), 34 (1992).
[5] P. M. Eleftherion, IEEE Electr. Insul. Mag. **11**(6), 22 (1995).
[6] H. J. Konle, M. Spitalny, C. O. Paschereit, F. Bake, I. Rohle, Meas. Sci. Technol. **21**(7), 075305 (2010).
[7] W. Wang, Q. Yu, X. Jiang, Optoelectron. Adv. Mat. **6**(7), 697 (2012).
[8] J. Chen, W. Li, H. Jiang, Microwave Opt. Technol. Lett. **54**(7), 1668 (2012).
[9] J. Posada-Roman, J. Rubio-Serrano, Sensors **12**(4), 4793 (2012).
[10] X. Wang, B. Li, Z. Xiao, S. H. Lee, H. Roman, O. L. Russo, K. K. Chin, K. R. Farmer, J. Micromech. Microeng. **15**(3), (2005).
[11] M. R. Islam, M. M. Ali, M. H. Lai, K. S. Lim, H. Ahmad, Sensors **14**(4), 7451 (2014).
[12] K. K. Chin, Y. Sun, G Feng, G E. Georgiou, K. Z. Guo, E. Niver, H. Roman, K. Noe, Appl. Opt. **46**(31), 7614 (2007).
[13] L. J. Song, Z. Wang, A. Wang, Y. L. Liu, K. L. Cooper, J. Lightwave Technol. **24**(9), 34338 (2006).
[14] S. Masoudi, G Amirian, E. Saeedi, M. Ahmadi, J. Mater. Eng. Perform. **24** (2), 3933 (2015).
[15] T. Grunder, A. Piquerez, M. Bach, P. Mille, J. Mater. Eng. Perform. **25**(7), 2914 (2016).
[16] Y. T. Yu, W. Z. Yuan, D. Y. Qiao, Q. Liang, Thin Solid Films **516**(12), 4070 (2008)
[17] A. Mitra, N. S. Prasad, G D. J. Ram, J. Mater. Eng. Perform **25**(4), 1384 (2016).
[18] C. Li, X. Gao, T. Guo, X. Jun, S. Fan, W. Jin, Meas. Sci. Technol. **26**(8), 085101 (2015).
[19] Z. C. Lin, W. L. Lai, H. Y. Lin, C. R. Liu, J. Mater. Process Tech. **97**(1), 200 (2000).
[20] M. MacAlpine, Z. Zhiqiang, M. S. Demokan, Electr. Pow. Syst. Res. **63**(1), 27 (2002).

*Corresponding author: yyt@nwpu.edu.cn